



Title	Synergistic role of retinoic acid signaling and Gata3 during primitive choanae formation
Author(s)	Kurosaka, Hiroshi; Mushiake, Jin; Mithun, Saha et al.
Citation	
Version Type	A0
URL	https://hdl.handle.net/11094/79001
rights	
Note	

The University of Osaka Institutional Knowledge Archive : OUKA

<https://ir.library.osaka-u.ac.jp/>

The University of Osaka

Synergistic role of retinoic acid signaling and Gata3 during primitive choanae formation

Hiroshi Kurosaka^{1*}, Jin Mushiaki¹, Saha Mithun¹, Yanran Wu¹, Qi Wang¹, Masataka Kikuchi², Akihiro Nakaya^{2,3}, Sayuri Yamamoto¹, Toshihiro Inubushi¹, Satoshi Koga⁴, Lisa L. Sandell⁵, Paul Trainor^{6,7}, Takashi Yamashiro¹.

1. Department of Orthodontics and Dentofacial Orthopedics, Graduate School of Dentistry, Osaka University

2. Department of Genome Informatics, Graduate School of Medicine, Osaka University

3. Laboratory of Genome Data Science Graduate School of Frontier Sciences, The University of Tokyo

4. Laboratory for Innate Immune Systems, RIKEN Center for Integrative Medical Sciences

5. Department of Oral Immunology and Infectious Diseases, University of Louisville School of Dentistry

6. Stowers Institute for Medical Research

7. Department of Anatomy and Cell Biology, University of Kansas School of Medicine

Author for correspondence

Hiroshi Kurosaka, DDS, PhD

kurosaka@dent.osaka-u.ac.jp

Associate Professor

Department of Orthodontics and Dentofacial Orthopedics, Graduate School of Dentistry, Osaka University

28 **Abstract**

29 Developmental defects of primitive choanae, an anatomical path to connect the embryonic nasal and
30 oral cavity, result in disorders called choanal atresia, which are associated with many congenital
31 diseases and require immediate clinical intervention after birth. Previous studies revealed that
32 reduced retinoid signaling underlies the etiology of choanal atresia. In the present study, by using
33 multiple mouse models which conditionally deleted *Rdh10* and *Gata3* during embryogenesis, we
34 showed that *Gata3* expression is regulated by retinoid signaling during embryonic craniofacial
35 development and plays crucial roles for development of the primitive choanae. Interestingly, *Gata3*
36 loss of function is known to cause hypoparathyroidism, sensorineural deafness and renal disease
37 (HDR) syndrome, which exhibits choanal atresia as one of the phenotypes in humans. Our model
38 partially phenocopies HDR syndrome with choanal atresia, and is thus a useful tool for investigating
39 the molecular and cellular mechanisms of HDR syndrome. We further uncovered critical synergy of
40 *Gata3* and retinoid signaling during embryonic development, which will shed light on novel
41 molecular and cellular etiology of congenital defects in primitive choanae formation.

42

Introduction

Craniofacial defects account for approximately 30% of all congenital anomalies, a rate largely due to the complexity of craniofacial development (1). Although the etiology and pathogenesis of cleft lip and/or palate are relatively well investigated (2), the developmental origins of many craniofacial anomalies are not well understood at either the molecular or cellular level. Choanal atresia (CA) is a craniofacial malformation characterized by a blocked nasal airway (3, 4). The incidence of CA is 1 in 5000 live births, and in cases of bilateral CA can be lethal. Therefore CA typically requires immediate intervention (5). In spite of this clinical significance, the basic etiology and pathogenesis of CA remains elusive. Although theoretical mechanisms have been proposed to explain the basis of choanal atresia, very little basic research using animal models has been performed, and conclusive answers have not been provided (6). It is well known that CA can occur in concert with various genetic disorders such as CHARGE syndrome and Crouzon syndrome (3). This indicates that multiple genetic pathways may underlie the development of primitive choanae formation and furthermore that disruption of these signaling pathways could result in CA. However, our knowledge of the interplay among molecular pathways during primitive choanae development is still rudimentary. In past studies, reduced retinoic acid signaling was proven to result in defects in primitive choanae formation and choanal atresia (4, 7). We previously identified multiple genes which exhibit significantly altered spatiotemporal patterns of expression in embryos with reduced

retinoic acid signaling (4). For example, the transcription factor *Gata3*, was significantly downregulated. *Gata3* is normally expressed at high levels in the developing facial processes during primitive choanae development in the normal situation, and interestingly, *GATA3* mutation in humans are associated with hypoparathyroidism, sensorineural deafness and renal disease (HDR) syndrome, which can also include craniofacial anomalies, such as CA (8-10). Multiple studies have investigated the role of *Gata3* in the parathyroid (11), cochlea (12, 13) and nephron duct (14) in order to determine the cellular and molecular mechanism underlying the development of each phenotype in HDR syndrome. In contrast, the pathogenesis of CA in HDR syndrome remains unknown. Here we generated tamoxifen-inducible *Gata3* knockout mice (*Ert2Cre:Gata3^{fx/fx}*) to elucidate the role of *Gata3* in craniofacial and primitive choanae development. We discovered that temporal excision of *Gata3* during embryonic frontonasal development resulted in reduced cell division of both epithelial and mesenchymal cells, which led to failure of the development of primitive choanae. We also uncovered a critical interaction between retinoid and *Gata3* function during craniofacial development, the disruption of which underlies the etiology of choanal atresia.

Results

Reduced *Gata3* expression is associated with choanal atresia (CA) in *Ert2Cre:Gata3^{fx/fx}* embryos

To discover signaling pathway(s) potentially involved in regulating primitive choanae formation, we analysed RNA-seq datasets we generated from the maxillary complex of E11.5 *Ert2Cre:Rdh10^{fx/fx}* and control littermate embryos, which exhibit CA (4). Putative protein interactome analyses were performed using the genes whose expression was either significantly reduced (blue) or elevated (red), with known associated proteins (green) (Figure 1A and B). From this analysis we detected several networks or clusters which included *Gata3* and whose expression was significantly reduced in *Ert2Cre:Rdh10^{fx/fx}* mice (Figure 1B). In parallel we also assessed the expression of *Gata3* in the frontonasal process of E11.5 embryos via *in situ* hybridization. While strong *Gata3* expression could be observed in the lambdoidal region in control E11.5 where the lateral nasal prominence (LNP), medial nasal prominence (MNP) and maxillary portion of the first pharyngeal arch (MXP), embryos, a substantial reduction was evident in E11.5 *Ert2Cre:Rdh10^{fx/fx}* embryos (Figure 1C and D). These results identified retinoid signaling as a candidate regulator of *Gata3* expression in the developing lambdoidal region, which anatomically presages the developing primitive choanae.

Expression pattern of *Gata3* mRNA and *RARE-LacZ* during primitive choanae formation

To further assess the correlation between *Gata3* expression and retinoid signaling during primitive choanae development, we performed *in situ* hybridization for *Gata3* in parallel with β galactosidase staining of *RARE-LacZ* embryos, which report retinoid signaling activity throughout the early stages

during frontonasal development. Strong *Gata3* expression was detected in the lambdoidal region in E11.0 embryos (Figure 2A). Frontal sections of stained embryos revealed that *Gata3* was expressed in both the epithelium and mesenchyme of the developing medial nasal and lateral nasal process at the position where the medial and lateral nasal processes were fusing (Figure 2B and D, red arrowhead). *RARE-LacZ* activity was detected around the developing lambdoidal region at E11.0 (Figure 2C), and frontal sections revealed an overlap of *RARE-LacZ* expression with *Gata3* expression at the junction where the medial and lateral nasal processes fuse (Figure 2B and D, red arrowhead). As development proceeded, the expression domain of *Gata3* became prominent specifically in the primitive choanae (Figure 2E, red arrowhead) and became restricted predominantly in the mesenchyme (Figure 2F). The expression of *RARE-LacZ* likewise became prominent around the primitive choanae at the E12.0 stage (Figure 2G) with intense retinoid signaling activity present in both the epithelium and mesenchyme (Figure 2H). The overlap in expression of *Gata3* and retinoid signaling around the primitive choanae (Figure 2F and H, red arrowhead), implying a synergistic role for these factors in regulating primitive choanae formation and development.

Elimination of *Gata3* disrupts formation of primitive choanae

To functionally test the global role of *Gata3* during primitive choanae formation, tamoxifen-

inducible *Gata3* knockout mice were produced by intercrossing *Gata3^{fx/fx}* mice (15) with *Ert2Cre* mice to generate *Ert2Cre:Gata3^{fx/fx}* mice (16). E9.5 tamoxifen treatment results in reduction but not elimination of intact *Gata3* in the developing choanae at E12.5 in *Ert2Cre:Gata3^{fx/fx}* embryos, as shown by *in situ* hybridization using RNA oligo probe against exon 4 of *Gata3* (Figure 3A and B). Tamoxifen administration at E9.5 results in 31% of *Ert2Cre:Gata3^{fx/fx}* embryos exhibiting either choanal atresia or choanal stenosis at E13.5 (Table 1). A further 34% were lethal at the same stage (Table 1). Some of the *Ert2Cre:Gata3^{fx/fx}* embryos presented with agenesis of the primitive choanae, while control *Gata3^{fx/fx}* littermates exhibited normal choanae development (Figure 3C-F). Frontal histological sections of *Ert2Cre:Gata3^{fx/fx}* embryos also confirmed the nasal cavity was blocked (Figure 3G and H). These results strongly indicate that *Gata3* expression during embryonic craniofacial development is critical for primitive choanae development, and that *Gata3* loss-of-function results in defects in primitive choanae formation.

Nasal cavity morphogenesis and shape are malformed in *Ert2Cre:Gata3^{fx/fx}* embryos

To further characterize malformation of the choanae and investigate the role of *Gata3* in nasal cavity formation, we generated three dimensional reconstructions of the volumetric shape of the nasal cavity in red and oral cavity in yellow. Micro CT scanning was therefore performed on both E13.5 control *Gata3^{fx/fx}* and *Ert2Cre:Gata3^{fx/fx}* embryos to which tamoxifen was administered at E9.5. The

shape of the nasal cavity was continuous from the nostril through the end of the nasal cavity and showed clear connection to the oral cavity in the control *Gata3^{fx/fx}* embryos (Figure 4A,B and C), whereas in mutant embryos, the nasal cavity was discontinuous and abnormally shaped and lacked the connection with the oral cavity (Figure 4D E and F). These results indicate that *Gata3* plays a critical role in primitive choanae formation as well as continuous nasal cavity development.

Reduced cell proliferation and increased cell death underly the etiology of CA, CS and nasal cavity deformation in *Ert2Cre:Gata3^{fx/fx}* mice

We previously revealed that reduced cell proliferation is a primary cause of CA during craniofacial development (4). We therefore assessed the pattern of cell proliferation during primitive choanae development via phosphorylated histone H3 (PHH3) immunostaining of sections through the frontonasal process. In control E11.5 embryos, both the nasal epithelium and craniofacial mesenchyme contained PHH3-positive cells (Figure 5A and B). The number of PHH3-positive cells was significantly reduced in *Ert2Cre:Gata3^{fx/fx}* embryos both in the epithelium and mesenchyme cells during nasal cavity development (Figure 5C-F). Moreover, the nasal epithelial cells were irregularly aligned at the position of invagination in *Ert2Cre:Gata3^{fx/fx}* embryos (Figure 5D). In parallel with analyses of alterations in proliferation we also examined the frontonasal processes for the induction of cell death. TUNEL staining revealed an endogenously low level of cell death in the

frontonasal process of control embryos (Figure 5G and H). In contrast, a significant elevation in the level of cell death was detected in both the frontonasal epithelium and mesenchyme in *Ert2Cre:Gata3^{fx/fx}* embryos (Figure 5I,J,K and L). These results indicate that *Gata3* regulates proliferation and cell survival which are crucial for normal primitive choanae and nasal cavity development. Interestingly, the overall spatiotemporal patterns of cell death and proliferation in *Ert2Cre:Gata3^{fx/fx}* embryos closely resembled that in *Ert2Cre:Rdh10^{fx/fx}* embryos (4). This further substantiates the notion that retinoid signaling and *Gata3* play central and perhaps synergistic roles in the development of the primitive choanae and nasal cavity.

Vitamin A deficient diet in dams results in early lethality of *Ert2Cre:Gata3^{fx/fx}* embryos

To test for synergy between retinoid signaling and *Gata3* function during embryogenesis, the pregnant dams of *Ert2Cre:Rdh10^{fx/fx}* embryos were placed on a vitamin A deficient diet from before mating and subsequently administered tamoxifen at E9.5 and the embryos were collected at E13.0. We observed a significant elevation in the incidence of developmental malformations, including lethality, in the *Ert2Cre:Gata3^{fx/fx}* embryos on a vitamin A deficient diet (Table 1). Most of the *Ert2Cre:Gata3^{fx/fx}* embryos whose mothers consumed a vitamin A deficient diet for more than 20 days showed signs of early lethality (no blood or heartbeat and opaque tissue, or resorption at E13.0) (Figure 6). Taken together, these results strongly suggest that retinoid signaling and *Gata3* function

act synergistically during embryogenesis to ensure embryo survival.

Discussion

Investigation of critical factors associated with retinoid signaling during primitive choanae formation

Multiple signaling pathways have been identified as key regulators of embryonic craniofacial development and retinoid signaling is one of the best studied molecular pathways (17, 18).

Eliminating *Rdh10*, a rate-limiting enzyme in the synthesis of retinoic acid causes severe craniofacial defects, including CA (4, 19, 20). Using a temporal conditional model of retinoid deficiency we previously identified a critical role for *Rdh10* and retinoid signaling in formation of the primitive choanae. (4). However, the molecular etiology of CA has not been fully elucidated and thus requires further investigation. From protein interactome analyses using the results obtained from RNAseq of *Rdh10* mutant and control embryo maxillary complexes (4), we discovered one network or cluster which pivoted on *Gata3* and exhibited significantly reduced expression (Figure 1A and B). Previous reports have shown that *Gata3* loss-of-function in mice results in early lethality around E11 with severe defects including craniofacial anomalies (21, 22). In addition, *GATA3* mutations in human result in hypoparathyroidism, sensorineural deafness and renal disease (HDR) syndrome, a constellation of anomalies that also includes craniofacial defects such as CA (8, 23). The fact that

Gata3 is strongly expressed around the developing frontonasal process in combination with its connection to human disease motivated us to investigate the role of *Gata3* in CA and its association with retinoid signaling (24). First, we confirmed a substantial reduction of *Gata3* expression around the developing primitive choana in E11.5 *Rdh10* mutant mouse embryos (Figure 1C and D). These results strongly suggest that retinoid signaling maybe responsible for activating *Gata3* in specific tissues during craniofacial development, especially around the primitive choana. Additionally, the spatiotemporal patterns of *Gata3* expression and *Rare-LacZ* reporter activity overlap during craniofacial development, especially around the frontonasal process. Notably, the ventral part of the developing nasal epithelium in the frontonasal process, a critical tissue for epithelial invagination and for forming oronasal membrane (3), co-expresses both *Gata3* and *Rare-LacZ* reporter (Figure 2B and D, red arrowhead). The overlapping expression of *Gata3* and *Rare-LacZ* reporter activity in the craniofacial epithelium implies a synergistic role for these molecular pathways in the process of primitive choanae development.

Disturbed expression of *Gata3* results in congenital defects including CA

To evaluate the functional role of *Gata3*, we utilized tamoxifen-inducible knock out mice (*Ert2Cre;Gata3^{fx/fx}*) in this study (16). Importantly, when tamoxifen was administered at E9.5, 31% (11/35) of the E13.5 *Ert2Cre;Gata3^{fx/fx}* embryos exhibited CA or choanal stenosis (CS) which

exhibit narrower primitive choanae (Table 1, Figure 3C-H). These results clearly demonstrate an essential role of *Gata3* in primitive choanae development. Interestingly, the expression of mRNA containing *Gata3* exon 4, which is located between the loxP sites, was not completely eliminated around the developing choanae (Figure 3A and B). Additionally, 34% (12/35) of E13.5 *Ert2Cre;Gata3^{fx/fx}* embryos exhibited early lethality. *Gata3* null mice are embryonic lethal around E11.5 (21). These results indicate that *Ert2Cre;Gata3^{fx/fx}* embryos retain some limited expression of *Gata3* which enables them to survive long enough to present with CA and CS at E13.5. The fact that the remaining 34% of *Ert2Cre;Gata3^{fx/fx}* embryos did not show either CA or CS suggests that there is a threshold level of *Gata3* expression required for normal primitive choanae development, below the defects occur.

The cytological role of *Gata3* in primitive choanae and nasal cavity development

Nasal cavity development requires continuous epithelial invagination and branching morphogenesis (25). Multiple genes and their pathways, such as *Fgf* and retinoid signaling, are known to be involved in this process (4, 26). In the present study, we discovered severe nasal cavity deformation in *Ert2Cre;Gata3^{fx/fx}* embryos (Figure 4). We also found a significant reduction of cell proliferation in both the epithelium and mesenchyme surrounding the developing nasal cavity (Figure 5A-F). Epithelial proliferation is one mechanism known to be critical for epithelial folding and branching

morphogenesis in various organs, such as the salivary glands and lungs (27). Interestingly, *Gata3* has been reported to play critical roles in ductal invasion during mammary gland development (28). In addition to alterations in proliferation significant elevation in cell death was also observed in *Ert2Cre;Gata3^{fx/fx}* embryos, especially in the ventral portion of the nasal cavity in the frontonasal processes (Figure 5G-L). Interestingly, a lack of retinoid signaling also causes similar cellular and developmental defects resulting in CA (4). These findings strongly suggest that *Gata3* regulates cell proliferation and cell survival in the developing nasal cavity, and this dysregulation of balance leads to nasal cavity defects, including CA and CS.

Synergistic effect of retinoid and *Gata3* signaling in embryonic development

To evaluate the synergistic effects of *Gata3* and retinoid signaling during frontonasal and choanae development, we reduced the level of retinoid signaling in *Ert2Cre;Gata3^{fx/fx}* embryos by administering vitamin A deficient food to pregnant dams. Interestingly, this experimental model resulted in an exaggerated malformation phenotype together with a significant increase in lethality (Table 1 and Figure 6). Interestingly, critical interactions between *Gata3* and retinoid signaling has been proposed for nephric duct insertion during kidney development (29). Our study however is the first report to show a critical interaction between *Gata3* and retinoid signaling during embryonic craniofacial development, especially in the etiology and pathogenesis of CA and CS. These insights

provide new knowledge about the contribution of *Gata3* to craniofacial development and advance our understanding of the molecular and cellular mechanisms underpinning CA and CS.

Material and Methods

Animals

Previously reported *Ert2Cre;Gata3^{flx/flx}* male mice were mated with *Gata3^{flx/flx}* female mice in order to get *Ert2Cre;Gata3^{flx/flx}* embryos (15, 16). *Rdh10^{flx/flx}* mice were derived from ES cells generated through KOMP and maintained as previously described (4, 20). These mice are equivalent to C57BL/6N-Rdh10^{tm1a(KOMP)Wtsi}. *Cre-ER^{T2}* (B6.129 Gt(ROSA)26Sortm1(cre/ERT2)Tyj/J, Jax stock #008463) from the Jackson Laboratory. For embryonic staging, the morning of identification of the vaginal plug was defined as E0.5. *Ert2Cre* and *Rare-LacZ* reporter mice were obtained from RIKEN BRC (STOCK Tg(RARE-Hspa1b/lacZ)12Jrt). Vitamin A deficient diet was purchased from CLEA Japan.

Protein interactome analysis

Mouse protein interactome data was obtained from the iRefIndex database (30). After interactions between the same genes (self-interactions) were removed, 46,512 interactions were

extracted. Among those interactions, 316 associations that interacted with the differentially expressed genes were visualized using Cytoscape software (31).

Administration of tamoxifen

In order to excise *Gata3* from the developing embryos, 40 ug/g-body of tamoxifen which was dissolved in 90% corn oil and 10% ethanol solution was administered by intraperitoneal injection of pregnant *Gata3*^{fx/fx} dams at E9.5.

Whole mount *in situ* hybridization

Whole-mount *in situ* hybridization of mouse embryos was performed as previously described (32). A minimum of three embryos of each genotype were examined per probe.

β-galactosidase staining

Staining for β-galactosidase expression in *RARE-lacZ* reporter mice was performed by fixing the tissue in 2% formaldehyde and 0.8% glutaraldehyde solution for 30 min at 4°C followed by treatment with 1mg/ml X-gal (Promega, # V3941) solution for 2 hours at room temperature.

274

275 **Whole-mount nuclear fluorescent imaging**

276 For analyzing choanal structure, the maxilla of the embryos were fixed in 4% PFA overnight at
277 4°C. Fixed tissue were washed several times in PBS and stained directly with DAPI (Dojindo)
278 (1:1,000) in PBS overnight at 4°C and visualized with a Olympus SZX16 stereomicroscope (33).

279

280 **Micro-CT analysis for evaluating the shape of nasal cavity**

281 The head of E12.5 embryos were stained with 0.3% phosphotungstic acid / 70% ethanol solution
282 overnight and scanned with an R_mCT2 (Rigaku) with 10 um slice pitch. The shape of the nasal
283 cavity was traced and the images were processed using ITK-SNAP (General Public License) for
284 3D reconstruction.

285

286 **Immunohistochemistry**

287 Antibodies against phospho-Histone-H3 (PHH3) (#05806, 1:200, Millipore) and E-Cadherin
288 (#3195, 1:200, Cell Signaling Technology) were used with appropriate secondary antibodies. Cell

death analysis was performed using the In Situ Cell Death Detection kit (Roche, #11684795910) following the manufacturer's instructions. The differences among the mean numbers of PHH3 and TUNEL positive cells in the epithelium and mesenchyme between control and *Ert2Cre;Gata3^{fx/fx}* embryos were evaluated by Student's two-tailed unpaired t-test. $P < 0.05$ indicated statistical significance.

Statistical analysis

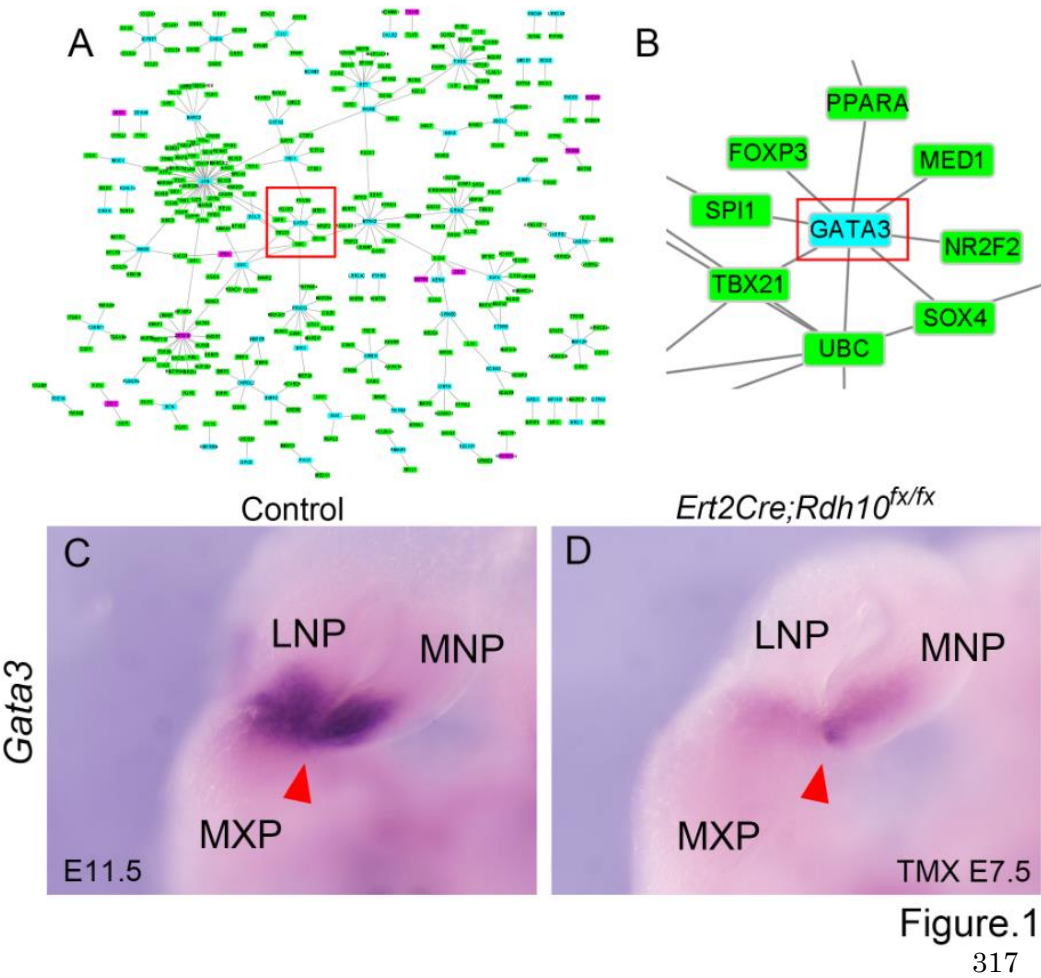
Two-proportion Z test was performed to evaluate the incidence of phenotypes (Table 1). $P < 0.05$ indicated statistical significance.

Acknowledgements

The authors thank the members of the Department of Orthodontics and Orthopedics, Graduate School of Dentistry, Osaka University, for their insights and comments throughout the project. The authors also deeply appreciate Dr. Sachiko Iseki at Tokyo Medical Dental University, Dr. Kazuyo Moro at RIKEN IMS and Dr. Jinfang Zhu for providing the animal models used in this research. The work was supported by grants-in-aid for scientific research from the Japan Society for the Promotion

305 of Science (#16K15836, 15H05687 and 19H03858 to HK). Research in the Trainor lab is supported
306 by the Stowers Institute for Medical Research.

307



318 **Figure.1. Reduction of RA signaling results in reduced *Gata3* expression during craniofacial**
319 **development.** (A) The result of protein interactome analysis using the dataset of genes whose
320 expression had been previously shown by RNAseq to be altered by reduced retinoid signaling (4).
321 (B) A cluster pivoting *Gata3*. (C) RNA *in situ* hybridization of *Gata3* in the developing maxillary
322 complex. Strong *Gata3* expression could be detected in the lambdoidal region of the developing
323 maxillary complex (red arrowhead). (D) Substantial reduction of *Gata3* mRNA expression could be

324 observed in the retinoid deficient *ErtCre:Rdh10^{flx/flx}* mutant to which tamoxifen was administered at

325 E7.5.

326

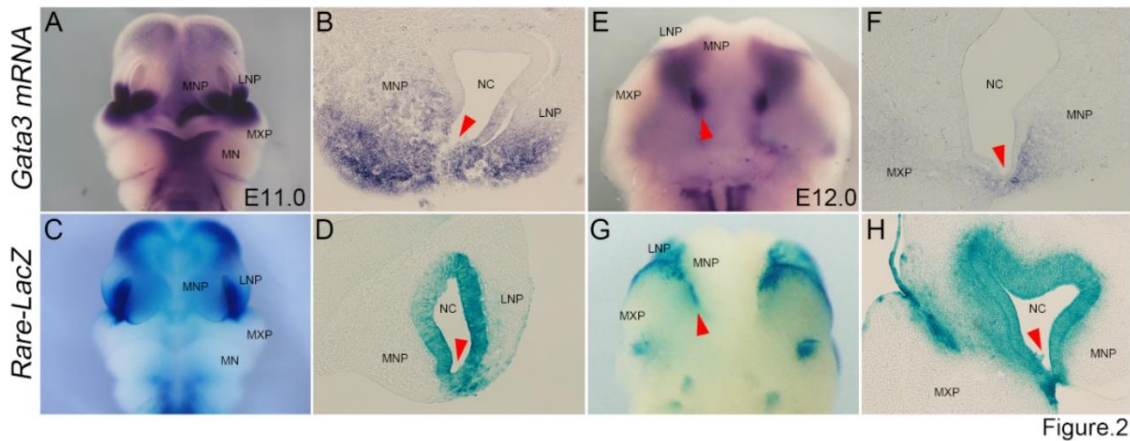


Figure.2.

327 **Figure 2. *Gata3* and retinoid signaling during frontonasal development. (A-F) *In situ***
 328 **hybridization of *Gata3* and (C-H) β galactosidase staining of the retinoid signaling reporter *Rare***
 329 ***LacZ* in developing head. Whole mount *in situ* hybridization for *Gata3* using embryonic head of**
 330 **E11.0 in frontal view (A) and E12.0 in ventral view (E). Frontal section of E11.0 (B and D) and**
 331 **E12.0 (F and H). Red arrowheads indicate the ventral epithelium of nasal cavity, which is important**
 332 **for primitive choanae formation. MNP, medial nasal process. LNP, lateral nasal process. MXP,**
 333 **maxillary process. NC, nasal cavity. MN, mandible.**

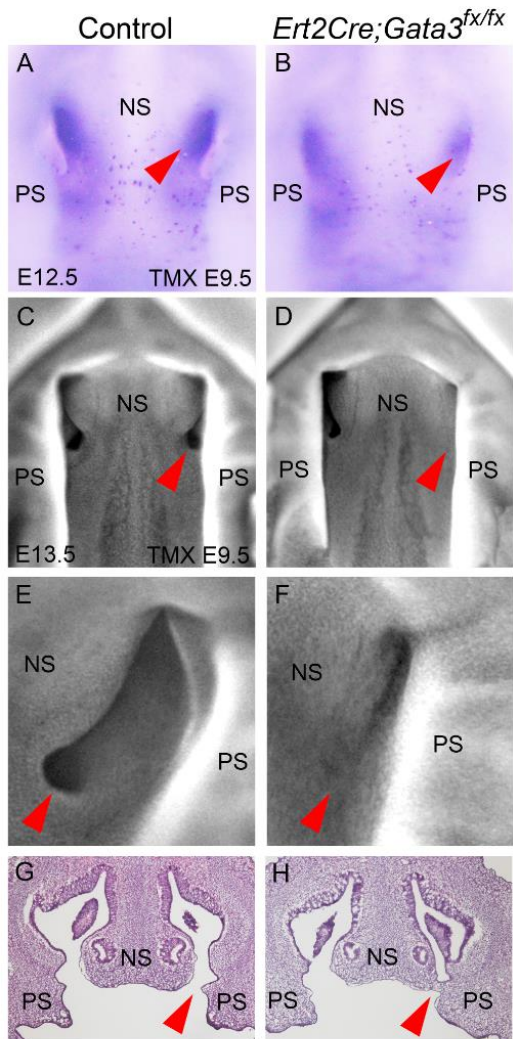


Figure.3.

Figure 3. Temporal reduction of Gata3 expression result in defects in primitive choanae

development. (A and B) *In situ* hybridization of exon 4 of *Gata3* at E12.5 in control (G) and

Ert2Cre;Gata3^{fx/fx} (H) embryos. (C-F) Ventral view of developing choanae in E13.5 maxilla in

control (C and E) and *Ert2Cre;Gata3^{fx/fx}* (D and F) embryos. (G and H) Hematoxylin and eosin

staining of frontal section of E13.5 heads in control (E) and *Ert2Cre;Gata3^{fx/fx}* (F) embryos. Red

arrowheads indicate the position of developing choanae. TMX, tamoxifen treatment.

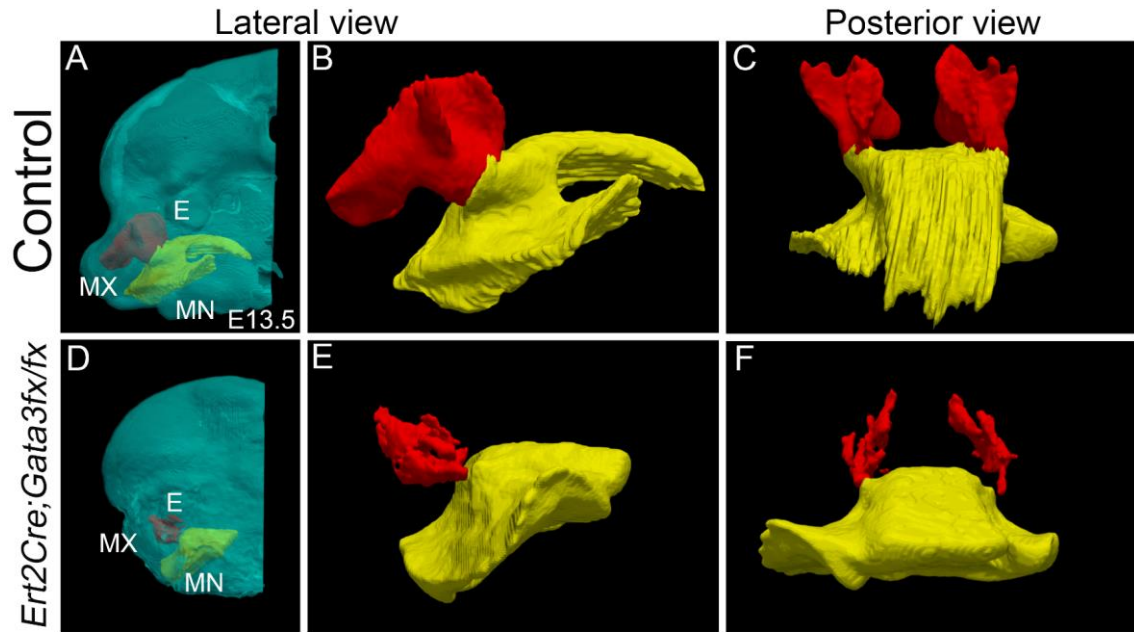


Figure.4

Figure 4. Three-dimensional reconstruction of the shape of developing nasal and oral cavity. (A and D) Overlaid image of reconstructed head surface (light green), and nasal (red) and oral (yellow) cavity seen from lateral view in E13.5 *Gata3^{fx/fx}* control (A) and *Ert2Cre;Gata3^{fx/fx}* (D) mouse to which tamoxifen was administered at E9.5 (B, C, E and F). 3-dimensional reconstruction of the shape of developing nasal (red) and oral (yellow) cavity in *Gata3^{fx/fx}* control (B and C) and *Ert2Cre;Gata3^{fx/fx}* (E and F) embryo. E, eye. MX, maxilla. MN, mandible.

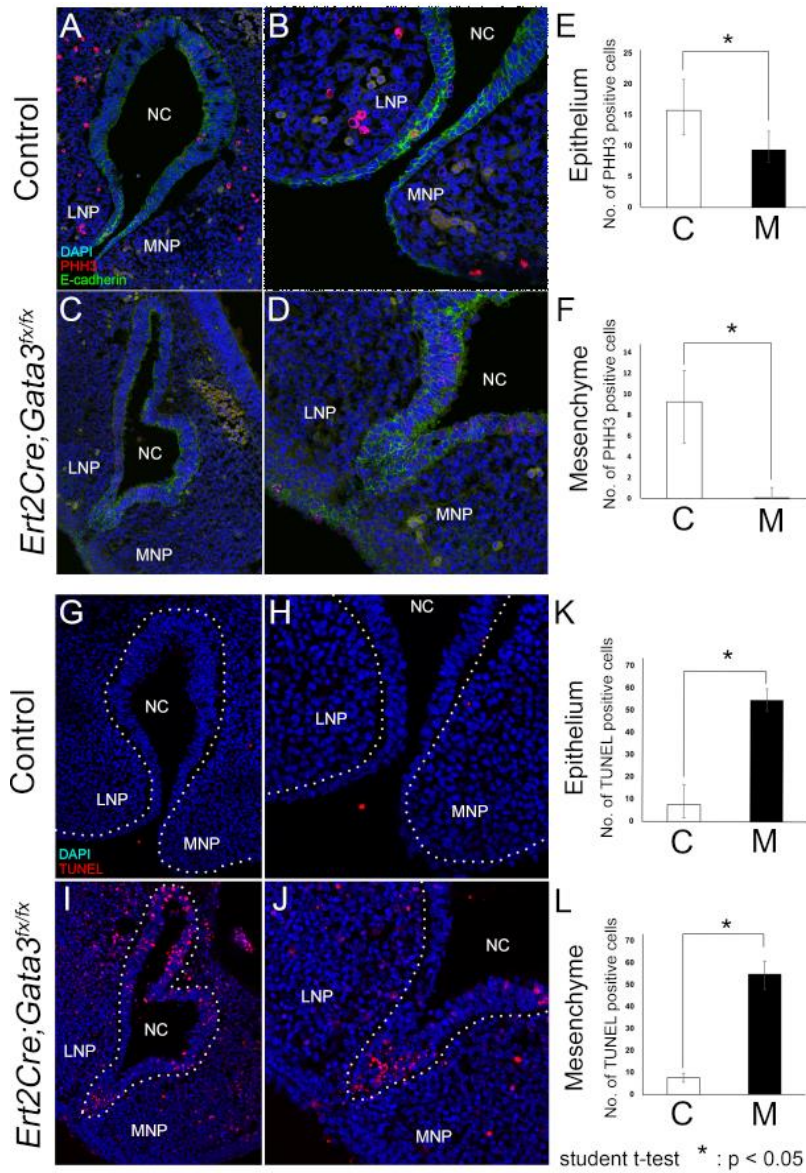


Figure.5.

Figure 5. Cell proliferation and death in the process of development of primitive choana. (A-D)

Immunohistochemistry of PHH3 (magenta) and E-CADHERIN (green) of frontal section of

developing nasal cavity in control (A and B) and *Ert2Cre;Gata3^{fx/fx}* embryos (C and D). (G-J)

TUNEL staining to detect cell death (magenta) in developing nasal cavity in control (G and H) and

Ert2Cre;Gata3^{fx/fx} (I and J) embryos. White dashed line indicates the boundary of nasal epithelium

367 and mesenchyme. B,D,H and J show magnified images of the ventral nasal cavity of A,C,G and
368 I, respectively. Statistical analysis was performed using the number of PHH3- (E and F) and
369 TUNEL-positive cells (K and L) in nasal epithelium and in the mesenchyme of nasal processes both
370 in control (white bar) and *Ert2Cre;Gata3^{flx/flx}* embryos (black bar). MNP, medial nasal process.
371 LNP, lateral nasal process. NC, nasal cavity. C, control. M, mutant (*Ert2Cre;Gata3^{flx/flx}*). Student T-
372 test $**P < 0.01$.
373

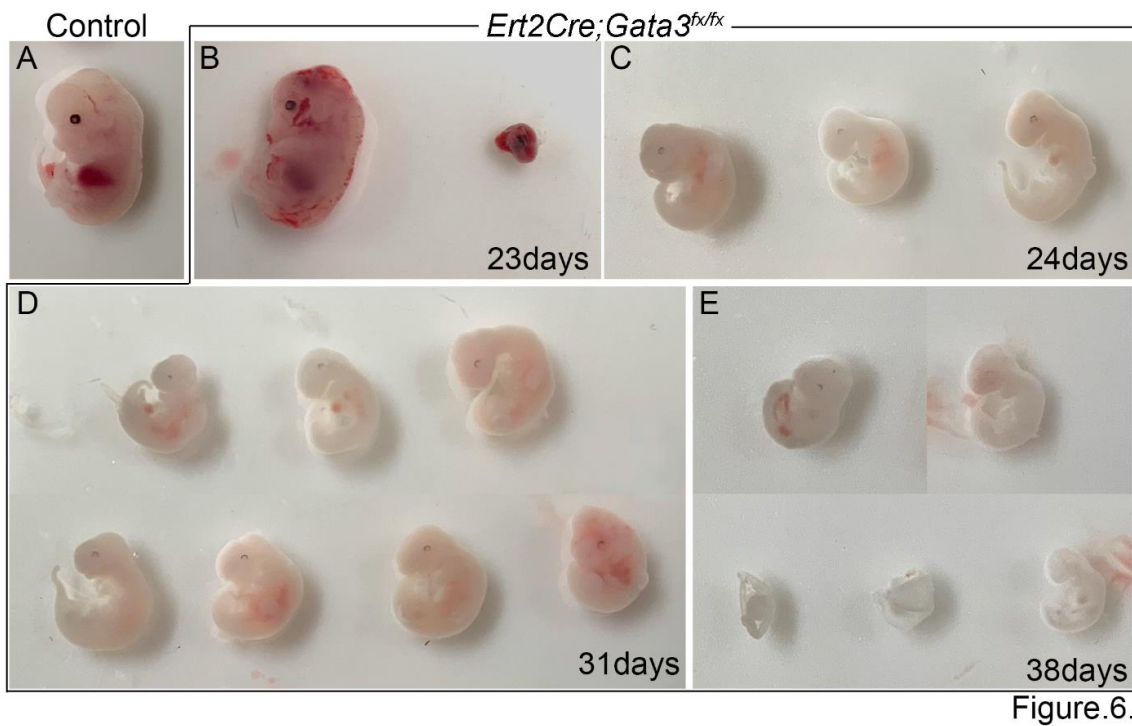


Figure.6.

Figure 6. Retinoid-deficient diet in *Ert2Cre;Gata3^{fx/fx}* embryos resulted in increased early lethality. (A) E13.0 control embryo with retinoid-deficient food for 38 days. (B-E)

Ert2Cre;Gata3^{fx/fx} embryos whose mother was fed retinoid-deficient food before fertilization. The days indicated in each figure show the duration of retinoid-deficient diet.

Table.1 Variation of the phenotype in present study

	Choanal Deformation (CA + CS)	Lethal	CD + Lethal	
<i>Gata3^{fx/fx}</i>	0% (0/50)	4% (2/50)	4% (2/50)	}
<i>Ert2Cre;Gata3^{fx/fx}</i>	31% (11/35)	34% (12/35)	66% (23/35)	
Vitamin A deficient <i>Gata3^{fx/fx}</i>	0% (0/14)	7% (1/14)	7% (1/14)	}
Vitamin A deficient <i>Ert2Cre;Gata3^{fx/fx}</i>	6% (1/17)	94% (16/17)	100% (17/17)	

CA, Choanal Atrasia; CS, Choanal Stenosis; CD, Choanal Deformation * : p<0.05

Table.1.

380

381

References

- 1 Trainor, P.A. and Andrews, B.T. (2013) Facial dysostoses: Etiology, pathogenesis and management. *Am J Med Genet C Semin Med Genet*, **163C**, 283-294.
- 2 Dixon, M.J., Marazita, M.L., Beaty, T.H. and Murray, J.C. (2011) Cleft lip and palate: understanding genetic and environmental influences. *Nat Rev Genet*, **12**, 167-178.
- 3 Kurosaka, H. (2019) Choanal atresia and stenosis: Development and diseases of the nasal cavity. *Wiley Interdiscip Rev Dev Biol*, **8**, e336.
- 4 Kurosaka, H., Wang, Q., Sandell, L., Yamashiro, T. and Trainor, P.A. (2017) Rdh10 loss-of-function and perturbed retinoid signaling underlies the etiology of choanal atresia. *Hum Mol Genet*, in press.
- 5 Kwong, K.M. (2015) Current Updates on Choanal Atresia. *Front Pediatr*, **3**, 52.
- 6 Lesciotto, K.M., Heuze, Y., Jabs, E.W., Bernstein, J.M. and Richtsmeier, J.T. (2018) Choanal Atresia and Craniosynostosis: Development and Disease. *Plast Reconstr Surg*, **141**, 156-168.
- 7 Dupé, V., Matt, N., Garnier, J.M., Chambon, P., Mark, M. and Ghyselinck, N.B. (2003) A newborn lethal defect due to inactivation of retinaldehyde dehydrogenase type 3 is prevented by maternal retinoic acid treatment. *Proc Natl Acad Sci U S A*, **100**, 14036-14041.
- 8 Barakat, A.J., Raygada, M. and Rennert, O.M. (2018) Barakat syndrome revisited. *Am J Med Genet A*, **176**, 1341-1348.
- 9 Barakat, A.Y., D'Albora, J.B., Martin, M.M. and Jose, P.A. (1977) Familial nephrosis, nerve deafness, and hypoparathyroidism. *J Pediatr*, **91**, 61-64.
- 10 Van Esch, H., Groenen, P., Nesbit, M.A., Schuffenhauer, S., Lichtner, P., Vanderlinden, G., Harding, B., Beetz, R., Bilous, R.W., Holdaway, I. *et al.* (2000) GATA3 haplo-insufficiency causes human HDR syndrome. *Nature*, **406**, 419-422.
- 11 Grigorieva, I.V., Mirczuk, S., Gaynor, K.U., Nesbit, M.A., Grigorieva, E.F., Wei, Q., Ali, A., Fairclough, R.J., Stacey, J.M., Stechman, M.J. *et al.* (2010) Gata3-deficient mice develop parathyroid abnormalities due to dysregulation of the parathyroid-specific transcription factor Gcm2. *J Clin Invest*, **120**, 2144-2155.
- 12 Duncan, J.S. and Fritzsch, B. (2013) Continued expression of GATA3 is necessary for cochlear neurosensory development. *PLoS One*, **8**, e62046.
- 13 Duncan, J.S., Lim, K.C., Engel, J.D. and Fritzsch, B. (2011) Limited inner ear morphogenesis and neurosensory development are possible in the absence of GATA3. *Int J Dev Biol*, **55**, 297-303.
- 14 Grote, D., Souabni, A., Busslinger, M. and Bouchard, M. (2006) Pax 2/8-regulated Gata 3 expression is necessary for morphogenesis and guidance of the nephric duct in the developing kidney.

416 *Development*, **133**, 53-61.

417 15 Zhu, J., Min, B., Hu-Li, J., Watson, C.J., Grinberg, A., Wang, Q., Killeen, N., Urban, J.F., Jr.,
 418 Guo, L. and Paul, W.E. (2004) Conditional deletion of Gata3 shows its essential function in T(H)1-T(H)2
 419 responses. *Nat Immunol*, **5**, 1157-1165.

420 16 Furusawa, J., Moro, K., Motomura, Y., Okamoto, K., Zhu, J., Takayanagi, H., Kubo, M. and
 421 Koyasu, S. (2013) Critical role of p38 and GATA3 in natural helper cell function. *J Immunol*, **191**, 1818-
 422 1826.

423 17 Metzler, M.A. and Sandell, L.L. (2016) Enzymatic Metabolism of Vitamin A in Developing
 424 Vertebrate Embryos. *Nutrients*, **8**.

425 18 Shannon, S.R., Moise, A.R. and Trainor, P.A. (2017) New insights and changing paradigms in
 426 the regulation of vitamin A metabolism in development. *Wiley Interdiscip Rev Dev Biol*, in press.

427 19 Sandell, L.L., Sanderson, B.W., Moiseyev, G., Johnson, T., Mushegian, A., Young, K., Rey,
 428 J.P., Ma, J.X., Staehling-Hampton, K. and Trainor, P.A. (2007) RDH10 is essential for synthesis of
 429 embryonic retinoic acid and is required for limb, craniofacial, and organ development. *Genes Dev*, **21**,
 430 1113-1124.

431 20 Sandell, L.L., Lynn, M.L., Inman, K.E., McDowell, W. and Trainor, P.A. (2012) RDH10
 432 oxidation of Vitamin A is a critical control step in synthesis of retinoic acid during mouse embryogenesis.
 433 *PLoS One*, **7**, e30698.

434 21 Pandolfi, P.P., Roth, M.E., Karis, A., Leonard, M.W., Dzierzak, E., Grosveld, F.G., Engel, J.D.
 435 and Lindenbaum, M.H. (1995) Targeted disruption of the GATA3 gene causes severe abnormalities in the
 436 nervous system and in fetal liver haematopoiesis. *Nat Genet*, **11**, 40-44.

437 22 Ruest, L.B., Xiang, X., Lim, K.C., Levi, G. and Clouthier, D.E. (2004) Endothelin-A receptor-
 438 dependent and -independent signaling pathways in establishing mandibular identity. *Development*, **131**,
 439 4413-4423.

440 23 Lemos, M.C. and Thakker, R.V. (2020) Hypoparathyroidism, deafness, and renal dysplasia
 441 syndrome: 20 Years after the identification of the first GATA3 mutations. *Hum Mutat*, **41**, 1341-1350.

442 24 Bonilla-Claudio, M., Wang, J., Bai, Y., Klysik, E., Selever, J. and Martin, J.F. (2012) Bmp
 443 signaling regulates a dose-dependent transcriptional program to control facial skeletal development.
 444 *Development*, **139**, 709-719.

445 25 Zwicker, D., Ostilla-Monico, R., Lieberman, D.E. and Brenner, M.P. (2018) Physical and
 446 geometric constraints shape the labyrinth-like nasal cavity. *Proc Natl Acad Sci U S A*, **115**, 2936-2941.

447 26 Kawauchi, S., Shou, J., Santos, R., Hébert, J.M., McConnell, S.K., Mason, I. and Calof, A.L.
 448 (2005) Fgf8 expression defines a morphogenetic center required for olfactory neurogenesis and nasal
 449 cavity development in the mouse. *Development*, **132**, 5211-5223.

450 27 Varner, V.D. and Nelson, C.M. (2014) Cellular and physical mechanisms of branching
 451 morphogenesis. *Development*, **141**, 2750-2759.

452 28 Kouros-Mehr, H., Slorach, E.M., Sternlicht, M.D. and Werb, Z. (2006) GATA-3 maintains the
 453 differentiation of the luminal cell fate in the mammary gland. *Cell*, **127**, 1041-1055.
 454 29 Chia, I., Grote, D., Marcotte, M., Batourina, E., Mendelsohn, C. and Bouchard, M. (2011)
 455 Nephric duct insertion is a crucial step in urinary tract maturation that is regulated by a Gata3-Raldh2-Ret
 456 molecular network in mice. *Development*, **138**, 2089-2097.
 457 30 Razick, S., Magklaras, G. and Donaldson, I.M. (2008) iRefIndex: a consolidated protein
 458 interaction database with provenance. *BMC Bioinformatics*, **9**, 405.
 459 31 Shannon, P., Markiel, A., Ozier, O., Baliga, N.S., Wang, J.T., Ramage, D., Amin, N.,
 460 Schwikowski, B. and Ideker, T. (2003) Cytoscape: a software environment for integrated models of
 461 biomolecular interaction networks. *Genome Res*, **13**, 2498-2504.
 462 32 Nagy, A. (2003) *Manipulating the mouse embryo : a laboratory manual*. Cold Spring Harbor
 463 Laboratory Press, Cold Spring Harbor, N.Y.
 464 33 Sandell, L.L., Kurosaka, H. and Trainor, P.A. (2012) Whole mount nuclear fluorescent
 465 imaging: convenient documentation of embryo morphology. *Genesis*, **50**, 844-850.
 466